Received Date : 17-Sep-2014
Revised Date : 22-Dec-2015
Accepted Date : 22-Dec-2015
Article type : Technical Paper

Author Manuscript

Applications of Explicitly-Incorporated/Post-Processing Measurement Uncertainty in Watershed Modeling

Haw Yen, Yamen Hoque, Xiuying Wang, Robert Daren Harmel

Assistant Research Scientist (**Yen**), Postdoctoral Fellow (**Hoque**), and Research Scientist (**Wang**), Blackland Research and Extension Center, Texas A&M Agrilife Research, 720 East Blackland Road, Temple, Texas 76502; and Supervisory Agricultural Engineer (**Harmel**), Grassland, Soil, & Water Research Laboratory, U.S. Department of Agriculture - Agricultural Research Service, Temple, Texas 76502 (E-Mail/Yen: hyen@brc.tamus.edu).

Abstract: In the field of watershed modeling, the impact of measurement uncertainty (MU) on calibration results indicates the potential issue of inaccurate model predictions. It is important to note MU refers to the uncertainty in measured data such as flow and nutrient values that are used to evaluate model outputs. The calculation of error statistics assuming measured data are deterministic may not be appropriate as has been frequently stated in literature. Although MU can affect model calibration results, it is rarely incorporated in modeling practice. MU can be incorporated in two schemes: explicitly-incorporated (MU-EI) during model calibration and post-processed (MU-PP) after calibration is completed. In this study, both schemes are implemented in a case study of the Arroyo Colorado Watershed, Texas, USA. Unexpectedly, no substantial differences were observed between each scheme for flow predictions. Although MU did not cause dramatic differences in most sediment and NH_4-N predictions, error statistics were affected in cases with MU greater than 50%, especially for sediment and NH_4-N. Therefore, it is

This is the author manuscript accepted for publication and has undergone full peer review but has not been through the copyediting, typesetting, pagination and proofreading process, which may lead to differences between this version and the Version of Record. Please cite this article as doi: 10.1111/1752-1688.12401-14-0199

This article is protected by copyright. All rights reserved

concluded MU may not exert a significant impact on model predictions until certain threshold is reached. This study demonstrates high levels of uncertainty in measured calibration/validation data significantly affect parameter estimation, especially in the auto-calibration process.

(Key Terms: Measurement uncertainty; Model calibration; SWAT; Uncertainty analysis; IPEAT.)

Author Manuscript

Introduction

In recent years, sophisticated watershed simulation models such as the Agricultural Policy/Environmental Extender Tool (APEX, Williams et al., 2012), Soil & Water Assessment Tool (SWAT, Arnold et al., 2012), and Hydrological Simulation Program-Fortran (HSPF, Bicknell et al., 1997) have been frequently applied to support water resources decision making. Hydrological and nutrient cycling processes represented by a large number of governing equations with model parameters have shown significant improvement in terms of the of model prediction accuracy (Yen et al., 2014c); however, calibration/validation (to define proper values of model parameter) has become computationally expensive as the calculation load has increased. To solve multi-dimensional problems and to make hundreds or even thousands of model simulations, a number of optimization techniques have been adopted and incorporated with auto-calibration tools (Duan et al., 1992; Tolson and Shoemaker, 2007; Vrugt et al., 2009; Yen et al., 2014a).

A major concern of traditional calibration processes is that the model uncertainty is either neglected (Balin et al., 2010) or assumed to be attributed only by model parameters (Ajami et al., 2007). Fortunately, there is increasing research work that explores contributions of and interactions among other sources of uncertainty. For example, the forcing input data (e.g., data used to be model inputs such as precipitation and temperature), measured calibration/validation data (MCVD, data used for model calibration and validation such as flow rate, sediment loads, etc.), and model structure should be considered in calibration and validation. Conclusions are made to support the idea that uncertainty sources exert considerable impact on model predictions (Ajami et al., 2007; Salamon and Feyen, 2009; Balin et al., 2010; Harmel et al., 2014; Yen et al., 2014c). Model predictions will be altered if varying sources of uncertainty are incorporated in

This article is protected by copyright. All rights reserved

watershed modeling. In addition, inappropriate decisions (e.g., unnecessary waste of financial resources) could be made if source(s) of uncertainty are disregarded (McMillan et al., 2011). In considering the importance of uncertainty, computational tools such as the Integrated Parameter Estimation and uncertainty Analysis Tool (IPEAT) have been developed to incorporate major sources of uncertainty including parameterization, input data, calibration/validation data, and model structural (Yen et al., 2014c). Scientists and stakeholders can take advantage of the modern techniques to conduct relevant studies or projects associated with broader impact.

Among the mentioned major uncertainty sources, parameter uncertainty has been studied extensively for the past two decades, and a large number of parameter uncertainty applications can be found in the literature (Osidele et al., 2006; Loosvelt et al., 2011). Measured input data are explored by using latent variables when input uncertainty was incorporated explicitly during auto-calibration (Kavetski et al., 2002; Ajami et al., 2007; Yen et al., 2014c). Structural uncertainty can be incorporated by using the Bayesian model averaging technique (BMA) where the posterior distributions are aggregated by BMA weights (Hoeting et al., 1999; Duan et al., 2007). A framework that can incorporate uncertainty in MCVD was developed and briefly examined in the applications of IPEAT (Yen et al., 2014c). However, detailed investigations of the impacts of measurement uncertainty on model predictions using auto-calibration techniques are still not fully explored.

It has been illustrated that uncertainty in MCVD should be considered in model evaluation (Harmel and Smith 2007; Harmel et al., 2010), but only few studies can be found on this topic because until recently few studies reported uncertainty in measured discharge and water quality data. Harmel and Smith (2007) and Harmel et al. (2010) also developed methods to consider measurement uncertainty in the calculation of error statistics. Theoretically, uncertainty in MCVD can be incorporated in two ways: explicitly incorporated (MU-EI) during auto-calibration (e.g., Yen et al., 2014c) or post-processed after the calibration is terminated/completed (MU-PP, Post-Processing scheme) (e.g., Harmel et al., 2010). Since the impact of uncertainty in MCVD in terms of MU-EI and MU-PP has not been evaluated, the goal of this study was to evaluate the impact of measurement uncertainty on applications of both Post-Processing and Explicitly-Incorporated schemes. The associated impact on calibration results and prediction uncertainty is quantified by considering the two schemes using pre-defined levels of measurement uncertainty (Harmel et al., 2006).

This article is protected by copyright. All rights reserved

Author Manuscript

Materials and Methods

SWAT Model

The Soil and Water Assessment Tool (SWAT) model was used to evaluate the impact of MU-EI and MU-PP on streamflow and water quality predictions. SWAT is a process-based, quasi-distributed, continuous time-step model that utilizes specific input data (topographic, soil, land-use/land-cover, weather, etc.) for the study domain to simulate the processes that constitute the hydrologic cycle, as well as sediment and nutrient transport and crop growth (Arnold et al., 2012). SWAT combines topographic (slope), soil property and land-cover attributes to divide a watershed into unique components called Hydrologic Response Units (HRUs). In any given sub-basin within the watershed being studied, model output such as runoff and water quality constituent loads are initially calculated at the HRU-scale, which are then summed to obtain the total contributions from each sub-basin to the stream reaches. SWAT has the capability to generate output for various water quality constituents (including but not limited to sediment, different forms of nitrogen and phosphorus, dissolved oxygen and pesticides) at a user specified time-step (sub-daily, daily, monthly or yearly). It has been shown to model agricultural watersheds with reasonable accuracy (Santhi et al., 2001) and continues to be one of the most widely used watershed models in the world (SWAT literature database, 2012; e.g., Fuka et al., 2014; Giacomoni et al., 2014; Park and Kim, 2014; Yen et al., 2014b).

Study Area and Input Data

Situated along the border of USA and Mexico, the Arroyo Colorado watershed (ACW) is a major sub-basin of the Nueces-Rio Grande Coastal Basin located in the Lower Rio Grande Valley, in southern Texas. The ACW has a drainage area of approximately 1,692 km^2, with the Arroyo Colorado River flowing eastward from the city of Mission to the Laguna Madre spanning portions of Hidalgo, Cameron, and Willacy counties. The watershed is predominantly agricultural (54% of total area) with grain sorghum, cotton, sugarcane, and citrus among the major cultivated crops. There has also been extensive urbanization (12.5% of area) in the western and central areas, along the main stem of the river where several cities (including Mission, McAllen, Pharr, Donna Weslaco, Mercedes, Harlingen, and San Benito) are located. Mostly clay, clay loam, and sandy loam soil types are prevalent within the watershed, with soil depths within the 1600-2000 mm range. Annual rainfall averages 530-680 mm, with an average annual

This article is protected by copyright. All rights reserved

Author Manuscript

temperature of 22.7 °C (mean monthly lows of 14.5 °C in January and 28.9 °C in July). A map of the watershed has been provided in Figure 2. Input data for the SWAT model of ACW include:

- Topographic: 30m resolution Digital Elevation Model (DEM) downloaded from the National Elevation Dataset (NED) maintained by the U.S. Geological Survey (USGS, accessible online at http://ned.usgs.gov/; last accessed on September 18, 2013).
- Land-Use: Land-use map created from remote sensing data and field surveys to represent land-cover conditions for 2004-2007 (Kannan 2012).
- Soil Properties: County-scale soil properties data acquired from the Soil Survey Geographic (SSURGO) database of USDA National Resources Conservation Service (NRCS) (accessible online at http://websoilsurvey.sc.egov.usda.gov/App/WebSoilSurvey.aspx; last accessed on September 18, 2013).

For this study the ACW was divided into 17 sub-basins, which where sub-divided into 475 HRUs. Crop management practices as well as best management practice (BMP) data (current and historical, from 1999-2006) were obtained from several sources including Texas A&M AgriLife Research, Texas Commission on Environmental Quality (TCEQ), Texas State Soil and Water Conservation Board (TSSWCB), and NRCS and Soil and Water Conservation District (SWCD) field offices (Table 1, details can be found in Kannan 2012). Weather data were collected from the Texas State Climatologist Office at College Station, Texas, for three stations located within the watershed (COOPID 419588 near Weslaco, COOPID 415836 near Mercedes, COOPID 413943 near Harlingen, see Figure 2). These data are comprised of daily precipitation and min/max air temperature for the four year period (2000-2003). The International Boundary and Water Commission provided daily streamflow data for two locations, the first near Llano Grando at FM 1015 (south of Weslaco) and the second near US 77 (south west Harlingen). Data for 21 permit-holding point source discharge locations were also collected. The point sources consisted of 16 municipal, three industrial, and two shrimp farm sites. Only limited water quality data were available for the watershed in the form of sparse grab samples for sediment and ammonium nitrogen (NH_4-N). In order to extend these data for use in this study, the software (LOADEST, Runkel et al., 2004) was used to convert them to monthly loads.

This article is protected by copyright. All rights reserved

Author Manuscript

Incorporation of Measurement Uncertainty

The primary objective of this study was to examine how model predictions can be affected by uncertainty in MCVD. The arbitrary data quality scenarios for MCVD ranged from worst to best case to represent uncertainty in measured streamflow, sediment, and NH_4-N (based on Harmel et al. (2006); summarized in Table 2). To adjust the error term, the probability distribution method detailed in Harmel and Smith (2007) was utilized. For each observed-predicted data pair, a correction factor was assigned to the error value:

$$E_k = \frac{CF_k}{0.5}\left(Q_k^{obs} - Q_k^{sim}\right) \quad (1)$$

Where, E_k is the adjusted error between observed (Q_k^{obs}) and simulated data (Q_k^{sim}) at time k; and CF_k is the correction factor at time k. CF_k is divided by 0.5 because that is the maximum probability of one half of the pdf, thus ensuring that the maximum value for CF_k is 0.5 as well.

The assumption being made is that the measurement uncertainty for each measured value is normally distributed, since that would enable its cumulative distribution function to be estimated with known mean and variance. The latter is computed as:

$$\sigma^2 = \begin{cases} \left(\frac{Q_k^{obs} - UB_k^{lower}}{\mu}\right)^2 \\ \left(\frac{UB_k^{upper} - Q_k^{obs}}{\mu}\right)^2 \end{cases} \quad (2)$$

Where, σ^2 is the variance of Q_k^{obs}; μ is the mean which contains a certain amount of the normal probability distribution (e.g. $\mu = \pm 3.9$ represents standard deviation which includes > 99.99% of a normal probability distribution); UB_k^{lower} and UB_k^{upper} are the upper and lower boundaries of every measured data point at time k which can be calculated as follows:

$$UB_k^{upper} = Q_k^{obs} + \frac{PER_k \cdot Q_k^{obs}}{100} \quad (3)$$

$$UB_k^{lower} = Q_k^{obs} - \frac{PER_k \cdot Q_k^{obs}}{100} \quad (4)$$

This article is protected by copyright. All rights reserved

Author Manuscript

Where, PER_k is the probable error range (PER) as reported by Harmel et al. (2006) at time k. Interested readers are directed to Harmel and Smith (2007) for details on error term modification and to Yen et al. (2014c) for details on implementation.

In this study measurement uncertainty is considered in model calibration during the calibration process (Explicitly-Incorporated, MU-EI) and following calibration (Post-Processing, MU-PP). Details on these methods appear subsequently.

Explicitly-Incorporated consideration of measurement uncertainty

The fundamental objective of model calibration is to minimize differences between simulated and observed data as represented by the error term. The error term in each model evaluation could be further adjusted while incorporating measurement uncertainty into the calibration process since MCVD is uncertain (Harmel et al., 2006; Yen et al. 2014c). As shown in Figure 1(A), MU-EI incorporates measurement uncertainty during automatic-calibration. Since auto-calibration generates proposed model parameters (that then serve as the new parameter set for the following iteration) based on previously derived best results (so that calibration results have better opportunity to be improved through generations), the solution of each current model run is determined by previously derived results as affected by measurement uncertainty (because "best" results are defined by the performance of statistics based on observation data that should not be identified as "deterministic" in practice). Therefore, the "optimal" parameter set may be potentially biased by the using MU-EI in auto-calibration optimization process. Although, ignoring measurement uncertainty as done in common practice also has many disadvantages (Harmel et al., 2006; 2009; Yen et al., 2014c).

Post-Processing consideration of measurement uncertainty

Instead of incorporating measurement uncertainty during the auto-calibration process (where results of all model generations will be affected by the incorporation of measurement uncertainty), MU-PP considers measurement uncertainty after auto-calibration is done, and only the best result based on is used to apply measurement uncertainty calculation (see Figure 1(B)). The MU-PP was in essence proposed by Harmel et al. (2010), who evaluated model performance with modified goodness-of-fit indicators. Thus in MU-PP, measurement uncertainty was not considered during calibration but instead was used to compare goodness-of-fit with and without incorporation of measurement uncertainty (and model uncertainty as well). However, it also

This article is protected by copyright. All rights reserved

Author Manuscript

means that MCVD (e.g., streamflow, sediment) were assumed to be deterministic while conducting calibration.

As described, MU-EI and MU-PP consider uncertainty in MCVD at different stages in calibration. The data quality scenarios applied with both MU-EI and MU-PP were used to investigate the impact on model predictions when measurement uncertainty is considered.

Description of Auto-Calibration Scenarios

In this study, 12 scenarios were evaluated (Table 2). Of these, scenarios MU-EI 01 and MU-PP 01 are typical calibration cases assuming no measurement uncertainty. The others are data quality scenarios from Harmel et al. (2006). MU-EI 02 and MU-PP 02 represent best case data quality scenarios with concentrated quality assurance/quality control (QA/QC) unconstrained by financial and personnel resource limitations and in ideal hydrologic conditions. MU-EI 03-05 and MU-PP 03-05 represent data collected with typical QA/QC under typical hydrologic conditions producing average values and maximum/minimum uncertainty boundaries to represent a 'typical' range of uncertainty. The final two scenarios, MU-EI 06 and MU-PP 06, represent the worst case for projects conducted with minimal attention to QA/QC, limited financial and personnel resources, and under difficult hydrologic conditions.

Model Calibration

The SWAT model for ACW was calibrated for a two year period (2002-2003) with streamflow calibration at a daily time-step and sediment and NH_4-N calibration at a monthly time-step. The Dynamically Dimensioned Search (DDS, Tolson and Shoemaker, 2007; Yen et al., 2014a) algorithm was used for auto-calibration. Since the observed data record was too short to be split into separate periods for calibration and validation, model validation was not conducted. However, this is justified because the study focused on evaluating the impact of measurement uncertainty on calibration results and not on matching model output to observed streamflow and water quality data.

Streamflow measured at the outlet of the watershed is impacted by the diurnal fluctuations of tidal waves stemming from the close proximity to the Gulf of Mexico. The ACW SWAT model was calibrated using data from a gage located near Llano Grande at FM 1015 to avoid the tidal effect. Streamflow data were available on a daily basis, but sediment and NH_4-N data were sparse; therefore, LOADEST was used to generate monthly sediment and NH_4-N data. Auto-

This article is protected by copyright. All rights reserved

Author Manuscript

calibration with the DDS algorithm modified 31 SWAT parameters that governed processes related to flow and water quality. These parameters and their recommended ranges are listed in Appendix A.

The Nash-Sutcliffe coefficient of efficiency (NSE) (Nash and Sutcliffe, 1970) was used to evaluate calibration performance. NSE normalizes the residual of error between observed and simulated against the mean observation. It is one of the most popular statistical measures to evaluate model performance (Servat and Dezetter, 1991; ASCE, 1993). The modified objective function can be seen in Equations 5 and 6:

$$NSE = 1 - \frac{\sum_{i=1}^{N}\left(y_i^{Obs} - y_i^{Sim}\right)^2}{\sum_{i=1}^{N}\left(y_i^{Obs} - y_i^{Mean}\right)^2} \quad (5)$$

$$OF = \sum_{v=1}^{V}\left(1 - NSE_v\right) \quad (6)$$

Where y_i^{Obs} is the observed response at time step i; y_i^{Sim} is the simulated response at time step i; y_i^{Mean} is the mean of observed response at time step i; and N is the total number of time steps. NSE equal to one indicates a perfect match between observation and simulation while a negative or small value of NSE indicates poor performance. As a result, the ideal global optimal solution for the OF during auto-calibration is defined such that it tends to be minimized at zero for a perfect match between measured and predicted values (i.e., NSE=1). OF is calculated as the sum of 1-NSE for the output variables (Equation 6), where OF is the final objective function value; NSE_v is the NSE value for output variable v; and V is the total number of output variables. For the current study, output variables stood for the constituents that were calibrated (streamflow, sediment, and NH_4-N). Please refer to Seo et al. (2014) for details on the modified objective function using NSE. The impact of measurement uncertainty on model prediction uncertainty was evaluated using inclusion rate and spread in accordance with Yen et al. (2014c). Inclusion rate is the percentage of observed data points located within the 95% confidence interval of the predicted outputs, while spread is the average width of corresponding uncertainty band around the predicted time-series.

Results and Discussion

Overall Performance of Automatic-Calibration by MU-EI & MU-PP

The overall performance of automatic-calibration by MU-EI for scenario MU-EI 01~06 is demonstrated in Figure 3. The goal of overall performance was to minimize *OF* as close to zero

This article is protected by copyright. All rights reserved

Author Manuscript

(perfect match) as possible. All scenarios converged earlier before maximum model runs (5,000 iterations) with similar patterns of convergence where fast convergence occurred before 2,000 run and no further improvement after. The range of minimum *OF* value was small, with values falling between 0.986-1.386 for the six scenarios. This implied that in terms of minimizing the overall *OF*, the level of uncertainty in MCVD has little impact auto-calibration. However, it can still be surmised that the smallest *OF* was achieved by scenario 6, which was the worst case scenario from Harmel et al. (2006). Intuitively, one might expect that *OF* values closest to zero would be likely achieved by Scenario 6 (the worst case scenario with larger measurement uncertainty) and the largest *OF* to be Scenario 1 without applying any measurement errors during calibration, but it is evidently not the case. On the other hand, differences of the final converged objective values among scenarios were larger than the absolute magnitudes. For example, MU-EI 06 was 17.5% lower than MU-EI 01, and the maximum variation (in comparing MU-EI 02 against MU-EI 06) was 40.6%. Therefore, more comparisons are demonstrated in the following section to evaluate the performance among varying levels of measurement uncertainty.

For MU-PP, the uncertainty in MCVD was not incorporated during auto-calibration but applied to the calibrated results "after" auto-calibration. In other words, error statistics were calculated using the same set of results from auto-calibration (as for MU-EI 01) but using different measurement uncertainty ranges as shown in Table 2.

Impacts on Adjusted Output Data via Error Statistics

Comparisons of MU-EI and MU-PP

As shown in Table 3 and Figure 4(A), 4(B), and 4(C), results of MU-EI indicate the following relative impacts of uncertainty in MCVD: streamflow < sediment < NH_4-N. On the other hand, different impacts were observed for MU-PP scenarios: streamflow < NH_4-N < sediment. Streamflow predictions (Figure 4(A)) do not show significant variations in terms of NSE values. For MU-EI scenarios, NSE decreases from 0.61 to 0.57, and it increases from 0.61 to 0.67 for MU-PP scenarios. As mentioned previously MU-EI incorporates uncertainty in MCVD ***DURING*** auto-calibration so that the converged results are affected by other solutions. Therefore, there is no guarantee that the incorporation of measurement uncertainty will provide better error statistics. In fact, error statistics may become worse (as shown in MU-EI of streamflow predictions). Meanwhile, there is no question that better results will be derived if measurement uncertainty increases in MU-PP scenarios because measurement uncertainty was

This article is protected by copyright. All rights reserved

Author Manuscript

only implemented ***AFTER*** the calibration is terminated. This does not mean, however, the mean error statistics will always declining if we apply MU-EI scheme. As shown in sediment and NH_4-N predictions (Table 3 and Figure 4(B), 4(C)), NSE values decreased (from MU-EI 01 to MU-EI 03 for both sediment and NH_4-N) but increased (from MU-EI 03 to MU-EI 05 for sediment and from MU-EI 03 to MU-EI 06 for NH_4-N). The results indicated that predictions are affected by conducting MU-EI, and the associated potential tendencies cannot be predicted through different levels of measurement uncertainty. It might be difficult for decision makers to consider measurement uncertainty during the decision making process. However, one should not disregard the fact that the existence of measurement uncertainty especially during the decision making process. Instead of assuming MCVD to be deterministic, the inclusion of uncertainty in MCVD with MU-EI realistically incorporates measurement uncertainty explicitly) in watershed simulation and the corresponding calibration processes.

Comparisons of MU-EI and traditional scheme (MU-EI-TD)

To examine the measurement uncertainty in detail, the MU-EI results for all scenarios were recalculated using the traditional approach (MU-EI-TD). By applying MU-EI-TD, the best results from MU-EI are recalculated without adding measurement uncertainty. Error statistics using MU-EI-TD are expected to be different than MU-EI. As shown in Figure 5(A), 5(B), and 4(C), the results presented previously were recalculated without incorporating measurement uncertainty, which means the MCVD were assumed to be completely deterministic in this case. In Figure 5(A), streamflow resulting from MU-EI and MU-EI-TD have negligible differences (measurement uncertainty ranges from ±3 to ±42%). However, considerable impact (Scenario 5 and 6) was found in sediment and NH_4-N predictions as shown in Figure 5(B) and 5(C), where the corresponding measurement uncertainty ranged from ±53 to ±177% for sediment and from ±100 to ±246% for NH_4-N. The comparisons between MU-EI and MU-EI-TD indicate two major findings. First, incorporation of measurement uncertainty does not exert substantial impact on calibration results for relatively low ranges (best case scenario, typical scenario minimum and typical scenario average defined by Harmel et al., 2006). Second, the best results (streamflow, sediment and NH_4-N processes) derived by MU-EI may have extensive differences compare to the scheme using traditional calculation. This does not imply whether MU-EI or MU-EI-TD is more superior to the other, but clearly identifies the need to consider potential impact for modeling applications.

This article is protected by copyright. All rights reserved

Author Manuscript

Comparisons by Using Behavior Definitions

Behavior definitions are statistical standards that represent the behavior of calibration results. Model performance can be evaluated by conceptual indices such as very good, good, satisfactory, and unsatisfactory (Yen et al., 2014b). In this study, the General Performance Ratings (Table 4) using NSE values (Moriasi et al., 2007) are taken as the reference of behavior definitions to identify model performance related to each scenario. As shown in Figure 6 and 7, no considerable differences can be found for streamflow predictions in all scenarios. The majority fell into the "Satisfactory" category 76.1~84.8% for MU-EI and 82.6~82.8% for MU-PP respectively where only a few solutions were "Good" (0.02~0.1% for MU-EI and 0.96~1.1% for MU-PP). For sediment and NH_4-N, substantial impact was found in Scenario 5 and 6 where statistics significantly improved with larger measurement uncertainty. Meanwhile, uncertainty in MCVD played a larger role in MU-EI than MU-PP. Dramatic increases of "Very Good" solutions occurred for MU-EI in Scenario 5 and 6 but more steady improvement was found in MU-PP. It is interesting to see that calibration results were affected more by MU-EI possibly because measurement uncertainty was incorporated throughout the calibration process; however, it could also indicate that MU-EI results are more biased.

Additional Information of MU-EI Scheme

Posterior distributions of predicted variables

Figures 8(A), 8(B), and 8(C) show the daily time-series of the best results for all six scenarios using MU-EI (daily streamflow and monthly sediment and ammonium-N, respectively). With the incorporation of measurement uncertainty into model calibration, it can be seen that particularly for sediment and ammonium-N, the time-series plots are quite divergent among the scenarios. However, if only the error statistics are examined, it gives the impression that the best calibration results are essentially analogous to each other. For example, for ammonium-N predictions in Figure 8(C) Scenarios 1 and 6 yielded comparable time-series even though the NSE scores (0.64 and 0.89) are quite different from each other. This may indicate that while calibration conducted in recent years have classified model performance based solely on error statistics such as NSE thresholds (e.g., model evaluation guidelines proposed by Moriasi et al., 2007), such an approach may be overrated, and further studies into evaluating model performance may be required.

This article is protected by copyright. All rights reserved

Author Manuscript

Prediction uncertainty and the associated impact

Table 5 is a summary of the inclusion rate (defined in this study as the percentage of observed data points located within the 95% confidence interval of the predicted outputs (Yen et al., 2014c)) of observed streamflow, sediment and ammonium-N. Table 5 also presents the spread (average width of corresponding uncertainty around the predicted time-series) by MU-EI. The units of spread for streamflow, sediment, and ammonium-N are cms (cubic meters per second), ton/ha (tons per hectare), and kg/ha (kilogram per hectare).

For streamflow, trend of inclusion rate and spread were similar. Both follow increase in measurement uncertainty in an irregular manner, increasing in some scenarios and descending in others. For example, Scenario 5 shows the highest inclusion rate and spread; however, the inclusion rate in Scenario 6 is fairly low compared to other scenarios. Results of sediment and ammonium-N predictions were different from streamflow since no significant variations occurred in spread (0.044-0.052 ton/ha for sediment and 0.136-0.147 kg/ha for ammonia). However, inclusion rates varied considerably, with Scenarios 4 and 5 yielding lowest and highest inclusion rates respectively for sediment. For ammonium-N, the highest inclusion rate occurred in Scenario 1 and Scenario 2 through 5 yielded the lowest.

Predictive uncertainty represented by the inclusion rate and average spread width was not examined to evaluate the advantage/disadvantage among scenarios. Case scenarios cannot be identified to be more or less superior by inclusion rate or spread (e.g., lower inclusion rate or narrower spread by increasing measurement uncertainty does not mean the performance is better/worse). Instead, they can be used to categorize model behavior (e.g., more or less prediction uncertainty by incorporating measurement uncertainty). It has been shown in this study that MU-EI incorporates measurement uncertainty while conducting automatic-calibration so that the results may not be predictable (but could be instead case sensitive). In short, the impact of measurement uncertainty on model predictions should be investigated in detail to avoid or reduce potential concerns (e.g., projected investment of conservation practices in a watershed may vary substantially with or without considering measurement uncertainty).

Conclusion

In this study, uncertainty in MCVD was investigated using MU-EI and MU-PP. For MU-EI, it is evident that higher level of measurement uncertainty (Scenario 5 and 6 in Figure 3) may result in better performance in terms of achieving improved objective function values. However,

This article is protected by copyright. All rights reserved

Author Manuscript

the best results from MU-EI at higher level of measurement uncertainty may also be more biased since a notable decline was observed by recalculating error statistics (see Figure 5). In comparing calibration results from MU-EI and MU-PP, no substantial influence was found for streamflow predictions. However, considerable differences were found in sediment and NH_4-N predictions especially when the measurement uncertainty is more than ±50%. In addition, MU-EI produced more change in terms of NSE and the rate of behavior solutions, which indicates that the MU-EI calibration process is influenced more by measurement uncertainty than MU-PP. On the other hand, the results do not specify a clear trend that solutions will be improved when applying MU-EI with higher level of measurement uncertainty (Table 4). The projected responses between automatic-calibration results using MU-EI versus MU-PP are still unpredictable.

The major goal of this study was not to determine whether MU-EI or MU-PP provides superior solutions for model calibration. Instead, the performances of two schemes demonstrate dissimilar behavioral definitions based on the Moriasi et al. (2007) categories. The inclusion of measurement uncertainty of MCVD within or after auto-calibration may cause varied and significant impact in calibration results and the resulting interpretations. For example, the national scale Conservation Effects Assessment Project (CEAP) conducted by the United State Department of Agriculture – Natural Resources Conservation Service (USDA-NRCS) categorized conservation needs into (i) High; (ii) Moderate; and (iii) Low (White et al., 2014). Each conservation scenario is defined by corresponding projected financial investment (USDA-NRCS, 2011a, b). Omission of measurement uncertainty in such simulations may dramatically affect estimated financial resource needs. Therefore, the proposed study provides a general concept for researchers, engineers, and modeling practitioners to use while conducting relevant decision making and model application.

[Insert Appendix A here]

Acknowledgements

This project was funded by grants from the United States Department of Agriculture - Natural Resources Conservation Service (USDA-NRCS) Conservation Effects Assessment Project (CEAP) - Wildlife and Cropland components.

This article is protected by copyright. All rights reserved

Author Manuscript

Literature Cited

Ajami, N. K., Duan Q., Sorooshian, S., 2007. An integrated hydrologic Bayesian multimodel combination framework: Confronting input, parameter, and model structural uncertainty in hydrologic prediction. Water Resources Research, 43(1), pp.1–19.

Amatya D. M., Jha, M. K., 2011. Evaluating the SWAT model for a low-gradient forested watershed in coastal south Carolina. Transactions of the ASABE, 54(6), pp.2151–2163.

Arnold, J., Moriasi, D., Gassman, P., Abbaspour, K., White, M., Srinivasan, Santhi, C., Harmel, R.D., van Griensven A., Van Liew M.W., Kannan N., and Jha, M. K., 2012. SWAT: Model use, calibration, and validation. Transactions of the ASABE, 55(4), 1491-1508.

Arnold, J. G., Allen, P. M., Bernhardt, G., 1993. A comprehensive surface-groundwater flow model, Journal of Hydrology, 142, 47–69.

Balin, D., Lee, H., Rode, M., 2010. Is point uncertain rainfall likely to have a great impact on distributed complex hydrological modeling. Water Resources Research, 46: doi: 10.1029/2009WR007848. issn: 0043-1397.

Bicknell, B. R., Imhoff, J. C., Kittle, Jr. JL., Donigian, A. S., Johanson, R. C., 1997. Hydrological Simulation Program--Fortran: User's manual for version 11. U.S. Environmental Protection Agency, National Exposure Research Laboratory, Athens, GA, EPA/600/R-97/080. 755 p.

Clark, M. P., Slater, A. G., Rupp, D. E., Woods, R. A., Vrugt, J. A., Gupta, H. V., Wagener, T., Hay, L. E., 2008. Framework for Understanding Structural Errors (FUSE): A modular framework to diagnose differences between hydrological models. Water Resources Research, 44, pp.1–14.

Duan, Q., Ajami, N. K., Gao, X., Sorooshian, S., 2007. Multi-model ensemble hydrologic prediction using Bayesian model averaging. Advances in Water Resources, 30(5), pp.1371–1386.

Duan, Q., Sorooshian, S., Gupta, V., 1992. Effective and efficient global optimization for conceptual rainfall-runoff models. Water Resources Research, 28(4), pp.1015–1031.

Fuka, Daniel R., M. Todd Walter, Charlotte MacAlister, Tammo S. Steenhuis, and Zachary M. Easton, 2014.SWATmodel: A Multi-Operating System, Multi-Platform SWAT Model

This article is protected by copyright. All rights reserved

Author Manuscript

Package in R. Journal of the American Water Resources Association, 50(5): 1439-1353. DOI: 10.1111/jawr.12170.

Gallagher, M., Doherty, J., 2007. Parameter estimation and uncertainty analysis for a watershed model. Environmental Modelling & Software, 22(7), pp.1000–1020.

Gassman, P. W., Reyes, M. R., Green, C. H., Arnold, J. G., 2007. The soil and water assessment tool: historical development, applications and future research directions, Transactions of the American Society of Agricultural and Biological Engineers 50 (4), 1211–1250.

Gesch, D., Evans, G., Mauck, J., Hutchinson, J., Carswell, Jr. W. J., 2009. The National Map—Elevation: U.S. Geological Survey Fact Sheet 2009-3053, 4 p. Last accessible online at http://ned.usgs.gov/; last accessed on September 18, 2013.

Giacomoni, M.H., R. Gomez, and E.Z. Berglund, 2014. Hydrologic Impact Assessment of Land Cover Change and Stormwater Management Using the Hydrologic Footprint Residence. Journal of the American Water Resources Association, 50(5): 1242-1256. DOI: 10.1111/jawr.12187

Harmel, R. D., Cooper, R. J., Slade, R. M., Haney, R. L., Arnold, J. G., 2006. Cumulative uncertainty in measured streamflow and water quality data for small watersheds. Transactions of the ASABE, 49(3), 689-701.

Harmel, R. D., Smith, P., 2007. Consideration of measurement uncertainty in the evaluation of goodness-of-fit in hydrologic and water quality modeling. Journal of Hydrology, 337(3-4), 326–336.

Harmel, R.D., Smith, D.R., King, K.W., Slade, R.M., 2009. Estimating storm discharge and water quality data uncertainty: A software tool for monitoring and modeling applications. Environmental Modelling & Software 24(7): 832-842.

Harmel, R. D., Smith, P. K., Migliaccio, K. W., 2010. Modifying goodness-of-fit indicators to incorporate both measurement and model uncertainty in model calibration and validation. Transactions of ASABE, 53(1), 55–63.

Harmel, R.D., Smith, P.K., Migliaccio, K.L., Chaubey, I., Douglas-Mankin, K., Benham, B., Shukla, S, Muñoz-Carpena, R., and Robson, B.J., 2014. Evaluating, interpreting, and communicating performance of hydrologic/water quality models considering intended use:

This article is protected by copyright. All rights reserved

Author Manuscript

A review and recommendations. Environ. Modeling Software 57: 40-51. doi.org/10.1016/j.envsoft.2014.02.013.

Hassan, A. E., Bekhit, H. M., Chapman, J. B., 2009. Using Markov Chain Monte Carlo to quantify parameter uncertainty and its effect on predictions of a groundwater flow model. Environmental Modelling & Software, 24(6), pp.749–763.

Hoeting, J. A., D. Madigan, A. E. Raftery, and C. T. Volinsky (1999), Bayesian Model Averaging : A Tutorial, Statistical Science, 14(4), 382-417.

Hoque, Y. M., Cibin, R., Hantush, M. M., Chaubey, I., Govindaraju, R. S., 2014. How do land use and climate change affect watershed health? A sceanrio-based analysis. Water Quality, Exposure and Health, 6(1-2), 19-33.

Kannan, N., Santhi, C., Williams, J. R., Arnold, J. G., 2007. Development of a continuous soil moisture accounting procedure for curve number methodology and its behaviour with different evapotranspiration methods. Hydrological Processes, 22(13), 2114–2121.

Kannan, N, 2012. SWAT Modeling of the Arroyo Colorado Watershed. Texas Water Resources Institute Technical Report No. 426.

Kavetski, D., Franks, S. W., Kuczera, G., 2002. Confronting input uncertainty in environmental modeling. Water Science and Application 6, pp.49–68.

Kavetski, D, Kuczera, G., Franks, S. W., 2006a. Bayesian analysis of input uncertainty in hydrological modeling: 1. Theory. Water Resources Research, 42(3), –9.

Kavetski D, Kuczera G, Franks SW (2006b) Bayesian analysis of input uncertainty in hydrological modeling: 2. Application. Water Resources Research, 42(3), 1–10.

Kuczera, G., Parent, R., 1998. Monte Carlo assessment of parameter uncertainty in conceptual catchment models: the Metropolis algorithm. Journal of Hydrology, 211(1-4), 69–85.

Loosvelt, L., Pauwels, V. R. N., Cornelis, W. M., De Lannoy, G. J. M., Verhoest, N. E. C., 2011. Impact of soil hydraulic parameter uncertainty on soil moisture modeling. Water Resources Research, 47(3), 1–16.

This article is protected by copyright. All rights reserved

Author Manuscript

McMillan, H., Jackson, B., Clark, M., Kavetski, D., Woods, R., 2011. Input Uncertainty in Hydrological Models: An Evaluation of Error Models for Rainfall . Journal of Hydrology 400(1-2): 83-94.

Moriasi, D. N., Arnold, J. G., Liew, M. W. V., Bingner, R. L., Harmel, R. D., and Veith, T. L., 2007. Model evaluation guidelines for systematic quantification of accuracy in watershed simulations, Transactions of the ASABE, 50(3), 885–900.

Nash, J.E., and Sutcliffe., J.V., 1970. River flow forecasting through conceptual models: Part I. A discussion of principles. J. Hydrol. 10(3): 282-290.

Neitsch, S. L., Arnold, J. G., Kiniry, J. R., Williams, J. R., 2011. Soil and Water Assessment Tool Theoretical Documentation Version 2009. Texas Water Resources Institute Technical Report No. 406, Texas A&M University System.

Osidele, O. O., Zeng, W., and Beck, M. B., 2006. A random search methodology for examining parametric uncertainty in water quality models. Water Science & Technology, 53(1), p.33.

Rains, T. H., Miranda, R. M., 2002. Simulation of Flow and Water Quality of the Arroyo Colorado, Texas, 1989-99, United States Geological Survey-Water Resources Investigations Report, No: 02-4110.

Park, Jong Y. and Seong J. Kim, 2014. Potential Impacts of Climate Change on the Reliability of Water and Hydropower Supply from a Multipurpose Dam in South Korea. Journal of the American Water Resources Association, 50(5): 1273-1288. DOI: 10.1111/jawr.12190

Refsgaard, J. C., van der Sluijs, J. P., Brown, J., van der Keur, P., 2006. A framework for dealing with uncertainty due to model structure error. Advances in Water Resources, 29(11), pp.1586–1597.

Runkel, R., Crawford, C., Cohn, T., 2004. Load Estimator (LOADEST): A Fortran Program for Estimating Constituent Loads in Streams and Rivers 2004. US Geological Survey Techniques and Methods Book, 4.

Salamon, P., Feyen, L., 2009. Assessing parameter, precipitation, and predictive uncertainty in a distributed hydrological model using sequential data assimilation with the particle filter. Journal of Hydrology, 376, 428-442, doi:10.1016/j.jhydrol.2009.07.051.

This article is protected by copyright. All rights reserved

Author Manuscript

Santhi, C., Arnold, J.G, Williams, J.R., Dugas, W.A., Srinivasan, R., and Hauck, L.M., 2001. Validation of the SWAT Model on A Large River Basin with Point and Nonpoint Sources, Journal of the American Water Resources Association, 37, 1169-1188.

Seo, M-J., Yen, H., Jeong, J., 2014. Transferability of input parameters between SWAT 2009 and SWAT 2012. Journal of Environmental Quality, 43, 869-880. doi: 10.2134/jeq2013.11.0450.

SWAT Literature Database Website, https://www.card.iastate.edu/swat_articles/, Last accessed 4/2/2014, 4:58 pm.

Tolson, B. A., Shoemaker, C. A., 2007. Dynamically dimensioned search algorithm for computationally efficient watershed model calibration. Water Resources Research, 43(1), pp.1–16.

USDA-SCS, 1972. National Engineering Handbook, Hydrology, Section 4, Chapter 4-10. Washington, D. C.: Soil Conservation Service.

USDA - Natural Resources Conservation Service, 2011a. Assessment of the effects of conservation practices on cultivated cropland in the Great Lakes region, Conservation Effects Assessment Project (CEAP). http://www.nrcs.usda.gov/Internet/FSE_DOCUMENTS/stelprdb1045480.pdf

USDA - Natural Resources Conservation Service, 2011b. Assessment of the effects of conservation practices on cultivated cropland in the Upper Mississippi River Basin, Conservation Effects Assessment Project (CEAP). http://www.nrcs.usda.gov/Internet/FSE_DOCUMENTS/stelprdb1042093.pdf

Vrugt, J. A., Braak, C. J. F., Diks, C. G. H., Robinson, B. A., Hyman, J. M., Higdon, D., 2009. Accelerating Markov Chain Monte Carlo Simulation by Differential Evolution with Self-Adaptive Randomized Subspace Sampling. International Journal of Nonlinear Sciences & Numerical Simulation, 10(March), 271–288.

White, M. J., Santhi, C., Kannan, N., Arnold, J. G., Harmel, R. D., Norfleet, L., Allen, P., DiLuzio, M., Wang, X., Atwood, J. D., Haney, E., Johnson, M., 2014. Nutrient delivery from the Mississippi River to the Gulf of Mexico and effects of cropland conservation. Journal of Soil and Water Conservation 69(1):26-40.

This article is protected by copyright. All rights reserved

Author Manuscript

Williams, J. W., Izaurralde, R. C., Steglich, E. M., 2012. Agricultural Policy/Environmental EXtender Model Theoretical Documentation Version 0806. 131 p.

Yen, H., Jeong, J., Tseng, W., Kim, M., Records, R., and Arabi, M., 2014a. Computational Procedure for Evaluating Sampling Techniques on Watershed Model Calibration. J. Hydrol. Eng. , 10.1061/(ASCE)HE.1943-5584.0001095 , 04014080.

Yen, H., Bailey, R. T., Arabi, M., Ahmadi, M., White, M. J., Arnold, J. G., 2014b. The Role of Interior Watershed Processes in Improving Parameter Estimation and Performance of Watershed Models. Journal of Environmental Quality, published online. doi:10.2134/jeq2013.03.0110

Yen, H., Wang, X., Fontane, D. G., Harmel, R. D., Arabi, M., 2014c. A framework for propagation of uncertainty contributed by parameterization, input data, model structure, and calibration/validation data in watershed modeling, Environmental Modelling and Software, 54, pp. 211-221, doi: 10.1016/j.envsoft.2014.01.004.

Yen, H., J. Jeong, S. Wang, S. Lu, M-K. Kim, Y-W. Su, 2015. Assessment of Model Configuration Effect by Alternative Evapotranspiration, Runoff, and Water Routing Functions on Watershed Modeling Using SWAT. Transactions of the ASABE, 57(4), pp. 1-13. DOI 10.13031/trans.58.10901

Author Manuscript

Table 1: Major best management practices (BMPs) implemented in the Arroyo Colorado Watershed (Kannan, 2012)

Best Management Practices	Highlights
Irrigation land leveling (NRCS practice code 464)	To reshape the irrigated land to a planned level to conduct efficient application of water
Irrigation Water Conveyance, Pipeline (NRCS practice code 430)	Installation of underground thermoplastic pipeline as a part of the irrigation system to replace canal lining.
Irrigation System-Surface Surge Valves	To replace on-farm ditches with pipeline with gates to distribute water to

This article is protected by copyright. All rights reserved

	irrigated fields
Irrigation Water Management (NRCS practice code 449)	Stakeholder will manage the frequency, and application rate of irrigation in considering federal, state, and local regulations
Conservation Crop Rotation (NRCS practice code 328)	To produce a minimum quantity of minimum residue one year within a given two year period
Nutrient Management (NRCS practice code 590)	To manage quantity, placement, and timing of fertilizers based on actual goals and moisture prospects
Residue Management (NRCS practice code 329b)	To manage the quantity, orientation, and distribution of different crop and residue from other plants on the soil surface while growing crops
Seasonal Residue Management (NRCS practice code 344)	Protective amounts of crop residue are secured on the soil surface through eroding period (critical) to reduce wind and water erosion during the raising of a high-residue crop
Terrace (NRCS Practice Code 600)	Implemented to conduct erosion control and water management
Constructed Wetlands	Free water surface systems were applied to aggregate effluent ponds at subbasin level
Wastewater Reuse	Wastewater used in irrigation to reduce point source nutrients to the river

Table 2: Measurement uncertainty represented by probable error ranges (PER) from Harmel et al. (2006)

Data Quality Scenarios	Streamflow (±%)	Sediment (±%)	NH_4-N (±%)	Explicitly-Incorporated Scenarios	Post-Processing Scenarios
No measurement uncertainty assumed	0[b]	0	0	MU-EI 01	MU-PP 01
Best case	3	3	3	MU-EI 02	MU-PP 02
Typical scenario minimum	6	7	11	MU-EI 03	MU-PP 03
Typical scenario average	10	18	31	MU-EI 04	MU-PP 04
Typical scenario maximum	19	53	100	MU-EI 05	MU-PP 05
Worst case scenario	42	117	246	MU-EI 06	MU-PP 06

Author Manuscript

This article is protected by copyright. All rights reserved

Author Manuscript

Table 3: NSE values for streamflow, sediment, and NH_4-N output for MU-EI and MU-PP scenarios

Scenario	NSE			Scenarios	NSE		
	Streamflow	Sediment	NH_4-N		Streamflow	Sediment	NH_4-N
MU-EI 01	0.61	0.74	0.64	MU-PP 01	0.61	0.74	0.64
MU-EI 02	0.58	0.64	0.60	MU-PP 02	0.61	0.74	0.64
MU-EI 03	0.58	0.64	0.60	MU-PP 03	0.61	0.74	0.64
MU-EI 04	0.58	0.67	0.64	MU-PP 04	0.61	0.77	0.67
MU-EI 05	0.57	0.78	0.74	MU-PP 05	0.66	0.85	0.71
MU-EI 06	0.57	0.77	0.89	MU-PP 06	0.67	0.92	0.78

NSE: Nash-Sutcliffe coefficient of efficiency (Nash and Sutcliffe, 1970)

Table 4: General performance ratings (Moriasi et al., 2007)

General Performance Rating	NSE
Very Good	$0.75 < NSE \leq 1.00$
Good	$0.65 < NSE \leq 0.75$
Satisfactory	$0.50 < NSE \leq 0.65$
Unsatisfactory	$NSE \leq 0.50$

NSE: Nash-Sutcliffe coefficient of efficiency

This article is protected by copyright. All rights reserved

Table 5: Inclusion rate of observed streamflow, sediment, and NH_4-N within the 95% confidence interval and the corresponding spread for the simulation period (2002-2003) by MU-EI

Scenario	Inclusion Rate[a]			Spread[b]		
	Streamflow (%)	Sediment (%)	NH_4-N (%)	Streamflow (m^3/s)	Sediment (ton/ha)	NH_4-N (kg/ha)
MU-EI 01	49.59	62.50	91.67	1.815	0.044	0.147
MU-EI 02	31.92	66.67	75.00	1.662	0.051	0.144
MU-EI 03	31.92	66.67	75.00	1.662	0.051	0.144
MU-EI 04	34.11	32.50	75.00	1.743	0.049	0.136
MU-EI 05	49.86	70.83	75.00	1.846	0.052	0.139
MU-EI 06	33.70	58.33	83.33	1.387	0.048	0.145

[a] Inclusion rate (%): Percentage of observed data points located within the 95% confidence interval.

[b] Spread: Average width of the corresponding uncertainty band along the predicted time series.

Author Manuscript

This article is protected by copyright. All rights reserved

List of Figures

Author Manuscript

This article is protected by copyright. All rights reserved

Appendix A - Calibration parameters for all case scenarios

Parameters	Input file	Units	Range	MU-EI 01	MU-EI 02	MU-EI 03	MU-EI 04	MU-EI 05	MU-EI 06	Description
ADJ_PKR	.bsn	-	0.5 – 2	0.93	0.89	0.92	0.94	1.00	0.98	Peak rate adjustment factor for sediment routing in the subbasin (tributary channels)
CMN	.bsn	-	0.001 – 0.003	0.0011	0.0027	0.0027	0.0028	0.0019	0.0021	Rate factor for humus mineralization of active organic nitrogen
EPCO	.bsn	-	0 – 1	0.52	0.72	0.72	0.53	0.54	0.68	Plant uptake compensation factor
NPERCO	.bsn	-	0 – 1	0.69	0.64	0.51	0.57	0.92	0.70	Nitrogen percolation coefficient
PRF	.bsn	-	0 – 2	0.52	0.70	0.70	0.79	0.62	0.68	Peak rate adjustment factor for sediment routing in the main channel
SPCON	.bsn	-	0.0001 – 0.01	0.0075	0.0097	0.0097	0.0074	0.0099	0.0096	Linear parameter for calculating the maximum amount of sediment that can be re-entrained during channel sediment routing
SPEXP	.bsn	-	1 – 1.5	1.00	1.35	1.35	1.31	1.31	1.46	Exponent parameter for calculating sediment re-entrained in channel sediment routing
SURLAG	.bsn	Day	1 – 24	6.17	4.89	4.89	3.38	7.99	4.32	Surface runoff lag time
SOL_NO3	.chm	mg/kg	0 – 100	1.77	4.24	4.24	1.18	2.31	1.77	Initial NO3 concentration in the soil layer
ALPHA_BF	.gw	1/Day	0 – 1	0.94	0.68	0.68	0.90	0.90	0.99	Baseflow alpha factor
GW_DELAY	.gw	Day	0 – 500	42.17	97.28	97.28	81.34	77.58	90.47	Groundwater delay
GW_REVAP	.gw	-	0.02 – 0.2	0.0375	0.0887	0.0887	0.0917	0.0634	0.0583	Groundwater "revap" coefficient
GWQMN	.gw	mm H_2O	0 – 5000	85.12	93.52	93.52	34.48	65.21	62.96	Threshold depth of water in the shallow aquifer required for return flow to occur
ESCO	.hru	-	0 – 1	0.74	0.97	0.97	0.99	0.80	0.71	Soil evaporation compensation factor
SLSUBBSN	.hru	M	10 – 150	53.36	70.53	70.53	59.10	63.28	70.56	Average slope length
CN_F	.mgt	%	±10	0.19	0.11	0.11	0.20	0.20	0.20	Initial SCS CN II value
USLE_P	.mgt	-	0 – 1	0.51	0.98	0.98	0.74	0.64	0.55	USLE equation support practice factor
CH_COV2	.rte	-	-0.001 – 1	0.44	0.35	0.35	0.39	0.25	0.32	Channel cover factor

Author Manuscript

This article is protected by copyright. All rights reserved

CH_K2	.rte	mm/hr	-0.01 – 500	6.15	3.43	3.43	5.54	2.84	2.84	Effective hydraulic conductivity in main channel alluvium
CH_N2	.rte	-	-0.01 – 0.3	0.09	0.11	0.11	0.11	0.08	0.07	Manning's "n" value for the main channel
SOL_AWC	.sol	%	±10	0.25	-0.20	-0.20	0.13	0.26	-0.03	Available water capacity of the soil layer
SOL_K	.sol	%	±10	0.19	0.29	0.27	0.25	0.20	0.08	Saturated hydraulic conductivity
USLE_K	.sol	%	±10	0.22	0.25	0.25	0.19	0.28	0.32	USLE equation soil erodibility (K) factor
CH_K1	.sub	mm/hr	0 – 300	42.44	77.42	77.42	70.76	58.61	64.50	Effective hydraulic conductivity in tributary channel alluvium
CH_N1	.sub	-	0.01 – 30	0.20	0.29	0.29	0.25	0.25	0.29	Manning's "n" value for the tributary channels
BC1	.swq	1/day	0.1 – 1	0.35	0.15	0.15	0.17	0.18	0.21	Rate constant for biological oxidation of NH4 to NO2 in the reach at 20°C
BC2	.swq	1/day	0.2 – 2	1.52	0.56	0.56	0.24	0.32	1.57	Rate constant for biological oxidation of NO2 to NO3 in the reach at 20°C
BC3	.swq	1/day	0.2 – 0.4	0.20	0.21	0.21	0.21	0.21	0.20	Rate constant for hydrolysis of organic N to NH4 in the reach at 20°C
RS3	.swq	mg/m^2-day	0 – 1	0.13	0.01	0.01	0.21	0.28	0.05	Benthic source rate for NH_4-N in the reach at 20°C
RS4	.swq	1/day	0.001 – 0.1	0.0973	0.0951	0.0951	0.0932	0.0962	0.0775	Rate coefficient for organic N settling in the reach at 20°C
USLE_C	crop.dat	%	±10	-0.0544	-0.2629	-0.2629	-0.2688	-0.2751	0.0926	Min value of USLE C factor applicable to the land cover/plant

Parameter values for CN_F, SOL_AWC, SOL_K, USLE_K, and USLE_C are the changes of fraction from default values.

Author Manuscript

This article is protected by copyright. All rights reserved

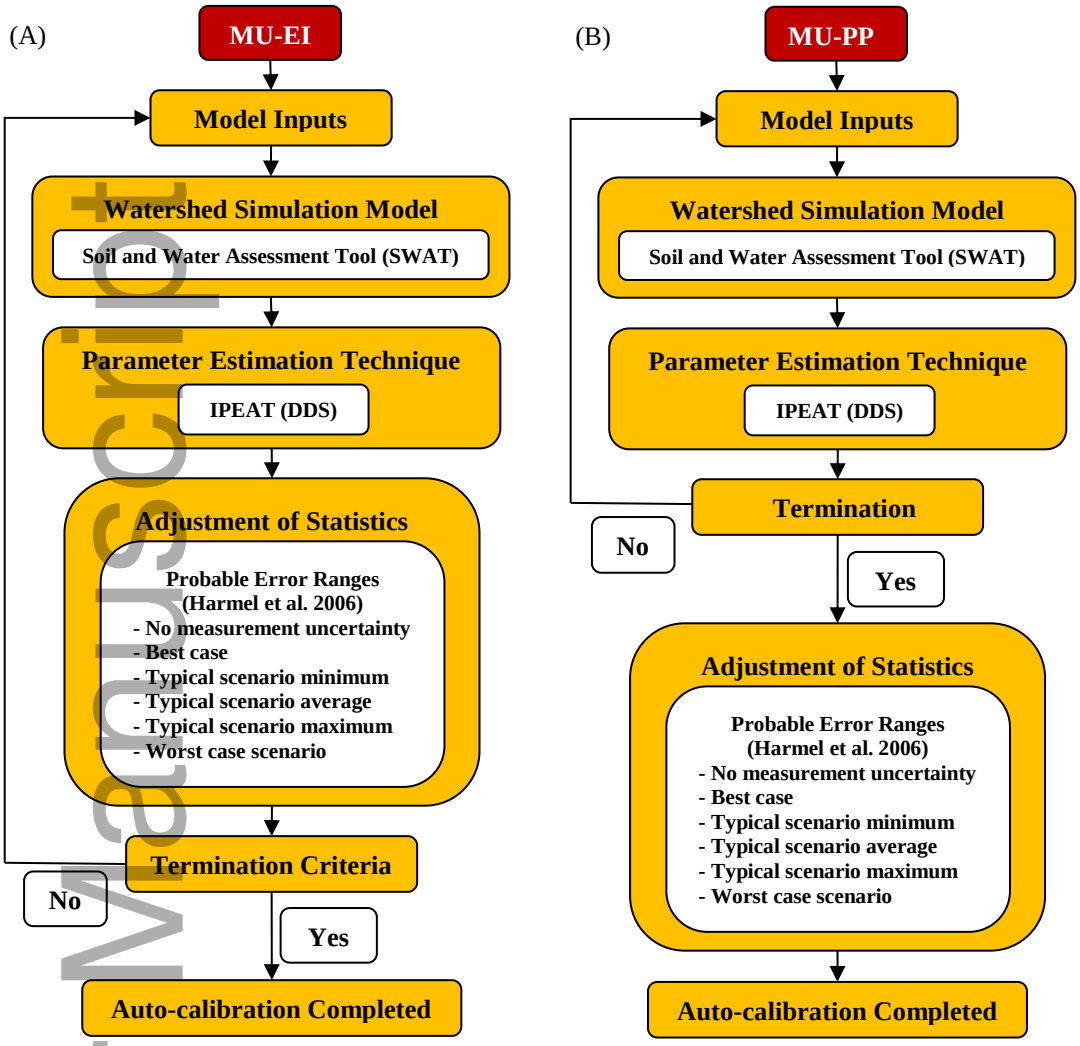

Figure 1. Organogram of two proposed approaches in incorporating measurement uncertainty: (A) Explicitly-Incorporated consideration of measurement uncertainty (MU-EI); and (B) Post-Processing consideration of measurement uncertainty (MU-PP)

Author Manuscript

This article is protected by copyright. All rights reserved

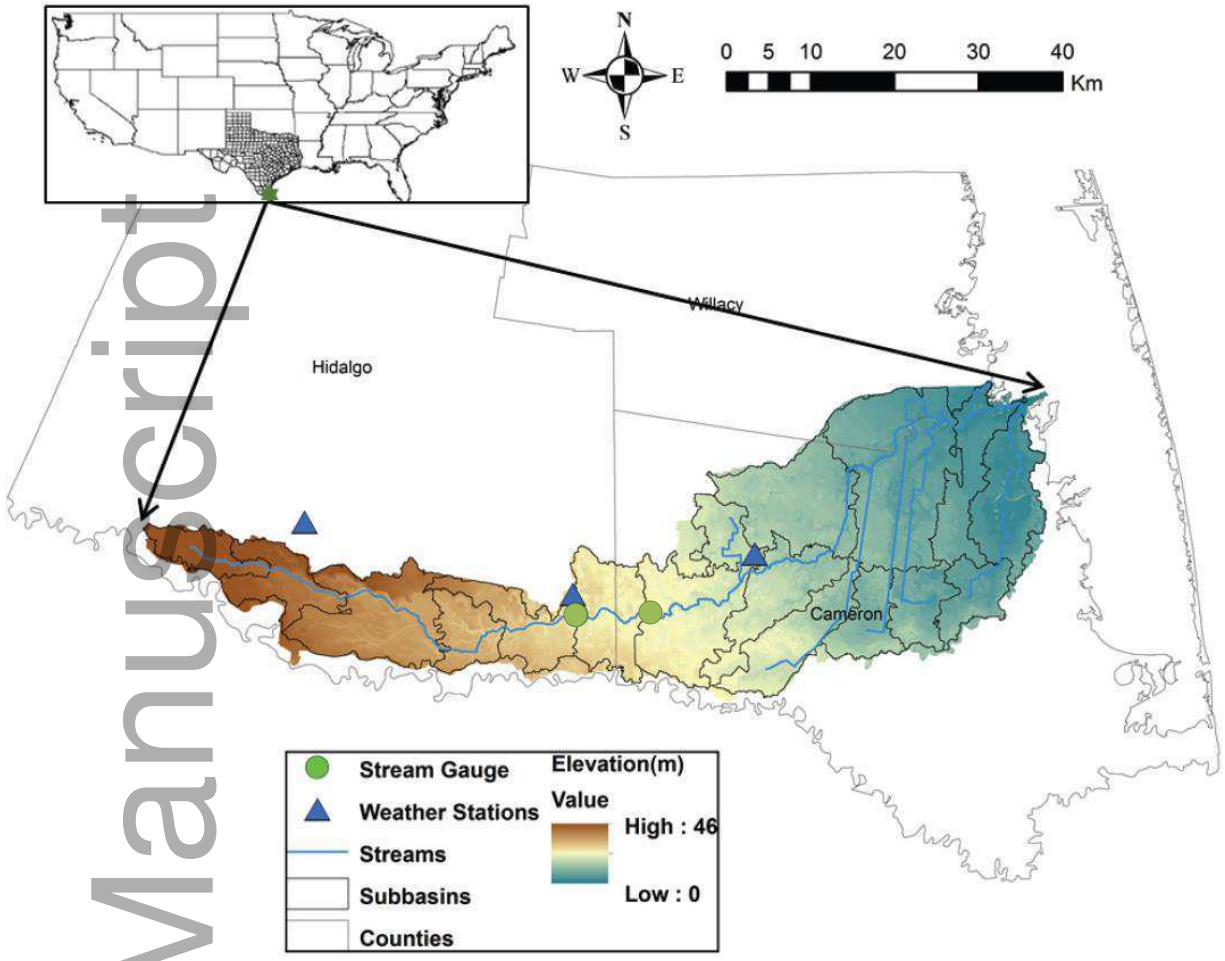

Figure 2. Location of the Arroyo Colorado Watershed (Yen et al., 2015)

Author Manuscript

This article is protected by copyright. All rights reserved

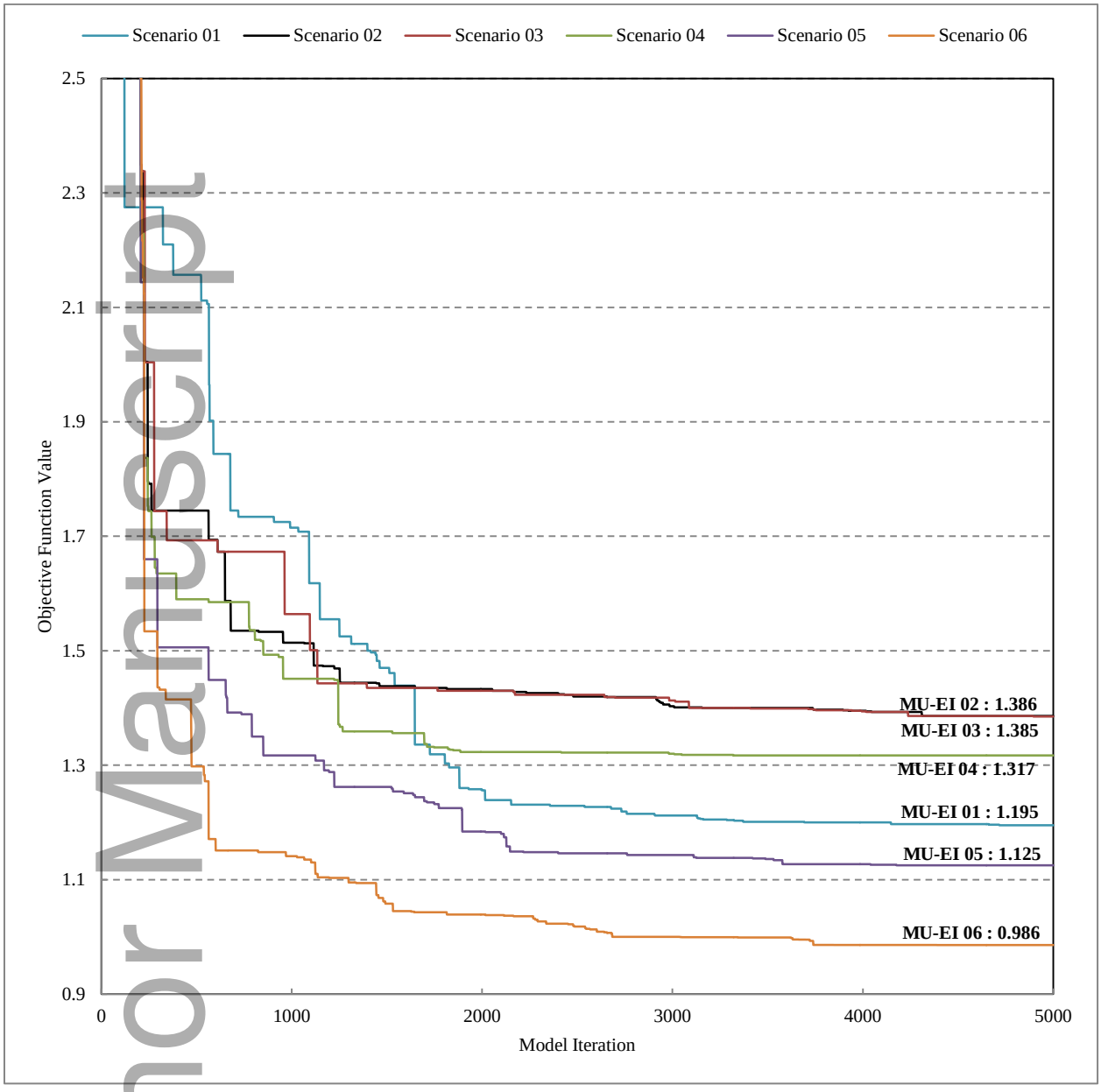

Figure 3. Objective function values and model convergence processes for MU-EI scenarios (e.g., the final converged objective function value for Scenario 01 is 1.195).

Author Manuscript

This article is protected by copyright. All rights reserved

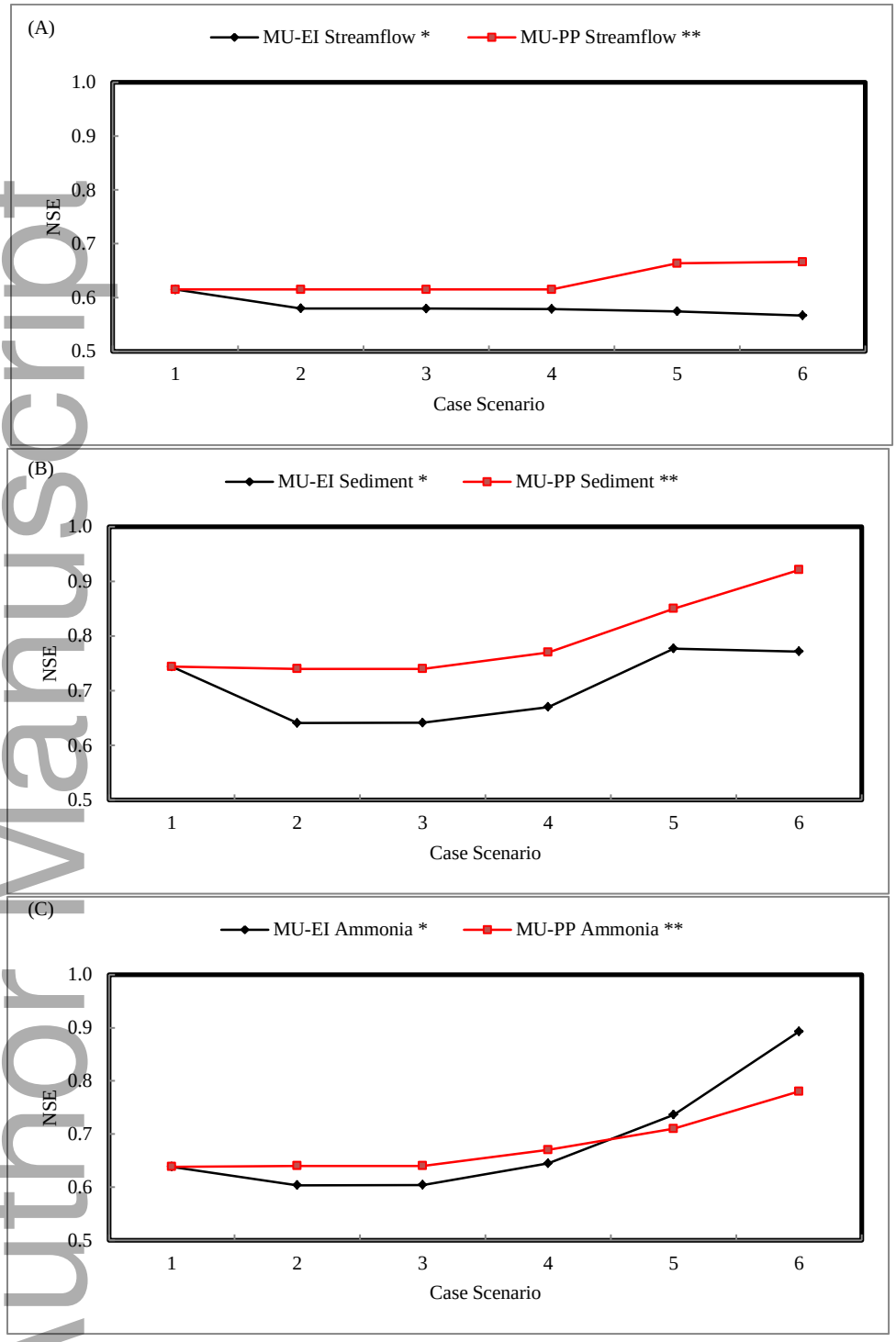

Figure 4. Demonstration of NSE values for output variables (streamflow/sediment/ammonia) of MU-EI (*: measurement uncertainty was incorporated explicitly during automatic-calibration) and MU-PP (**: measurement uncertainty was applied using post-processing scheme).

Author Manuscript

This article is protected by copyright. All rights reserved

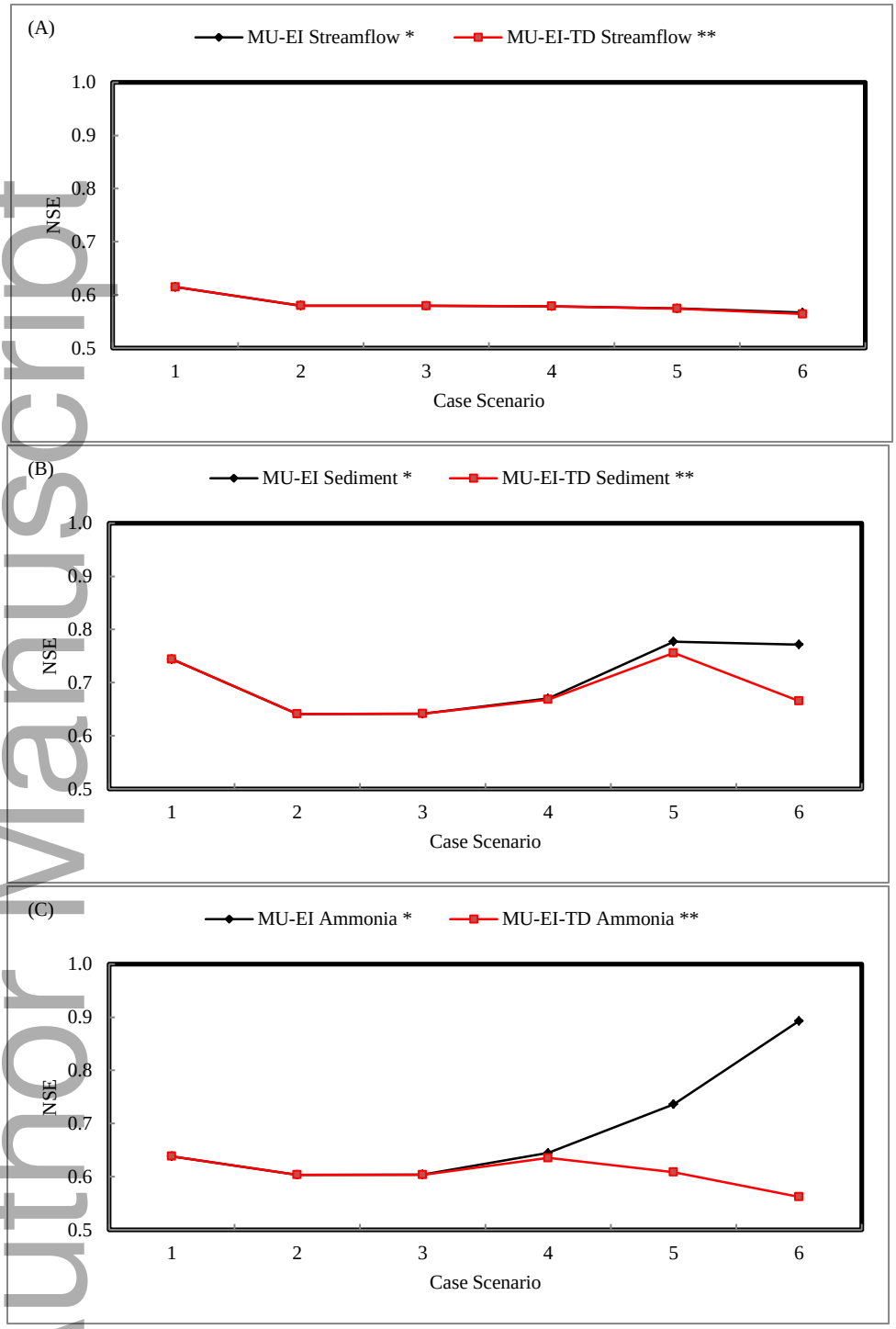

Figure 5. Demonstration of NSE values for output variables (streamflow/sediment/ammonia) of MU-EI (*: measurement uncertainty was incorporated explicitly during automatic-calibration) and MU-EI-TD (**: results from MU-EI were recalculated without including measurement uncertainty equations).

Author Manuscript

This article is protected by copyright. All rights reserved

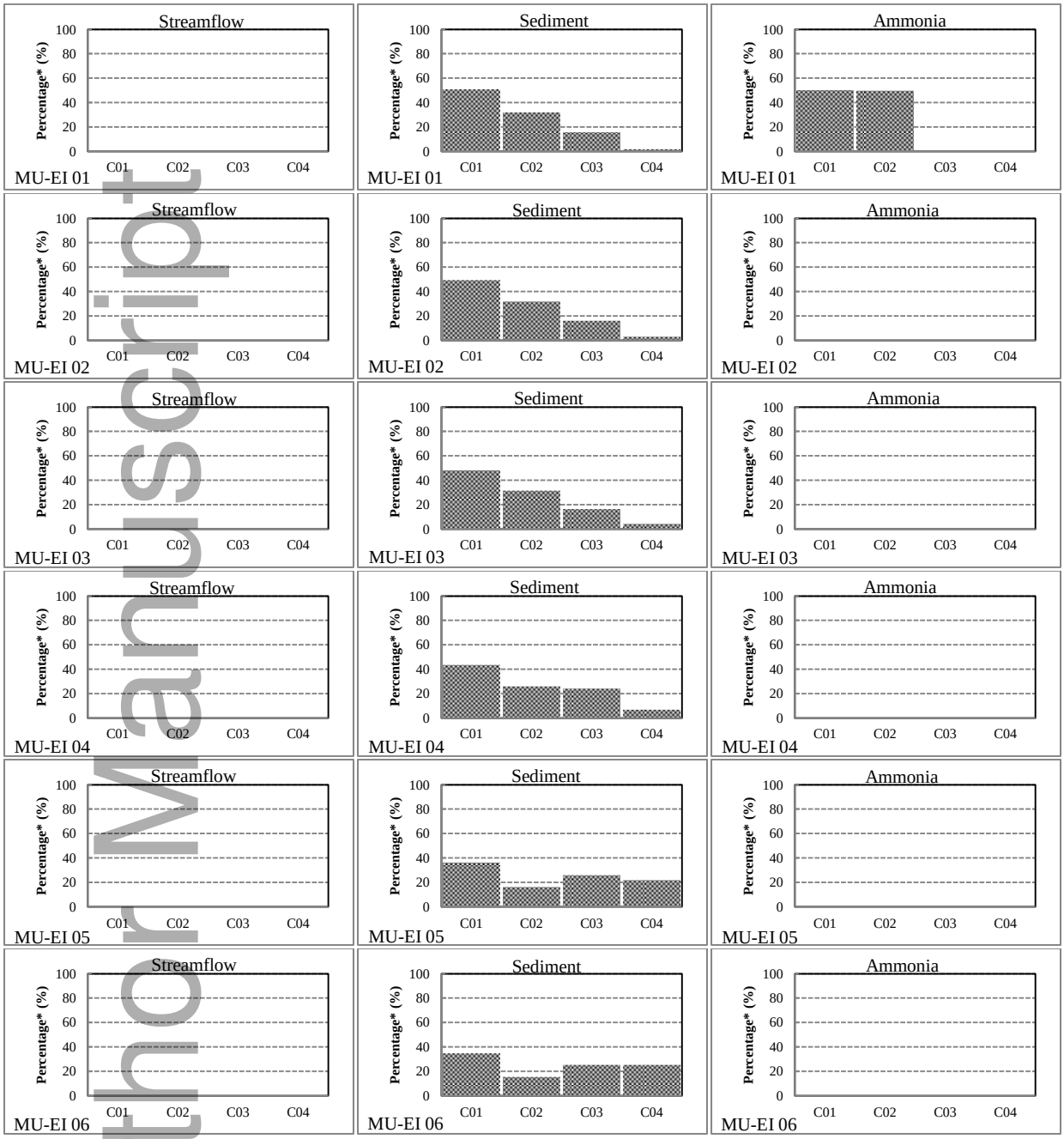

C01: "Unsatisfactory"
C02: "Satisfactory"
C03: "Good"
C04: "Very Good"

Figure 6. Behavior solutions (represented in percentage) by applying the General Performance Ratings (Moriasi et al., 2007) for MU-EI scheme.

Author Manuscript

This article is protected by copyright. All rights reserved

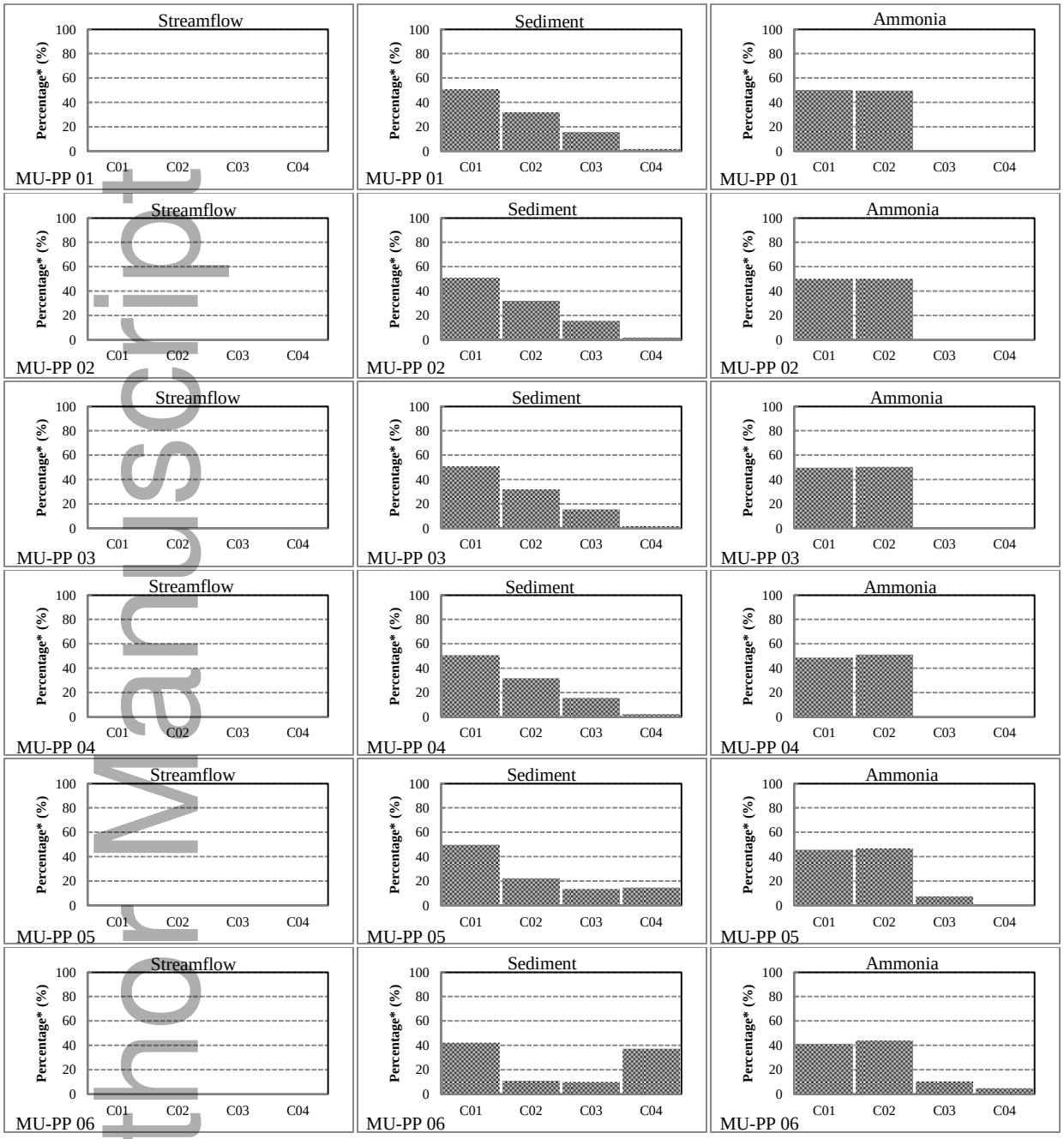

C01: "Unsatisfactory"
C02: "Satisfactory"
C03: "Good"
C04: "Very Good"

Figure 7. Behavior solutions (represented in percentage) by applying the General Performance Ratings (Moriasi et al., 2007) for MU-PP scheme.

Author Manuscript

This article is protected by copyright. All rights reserved

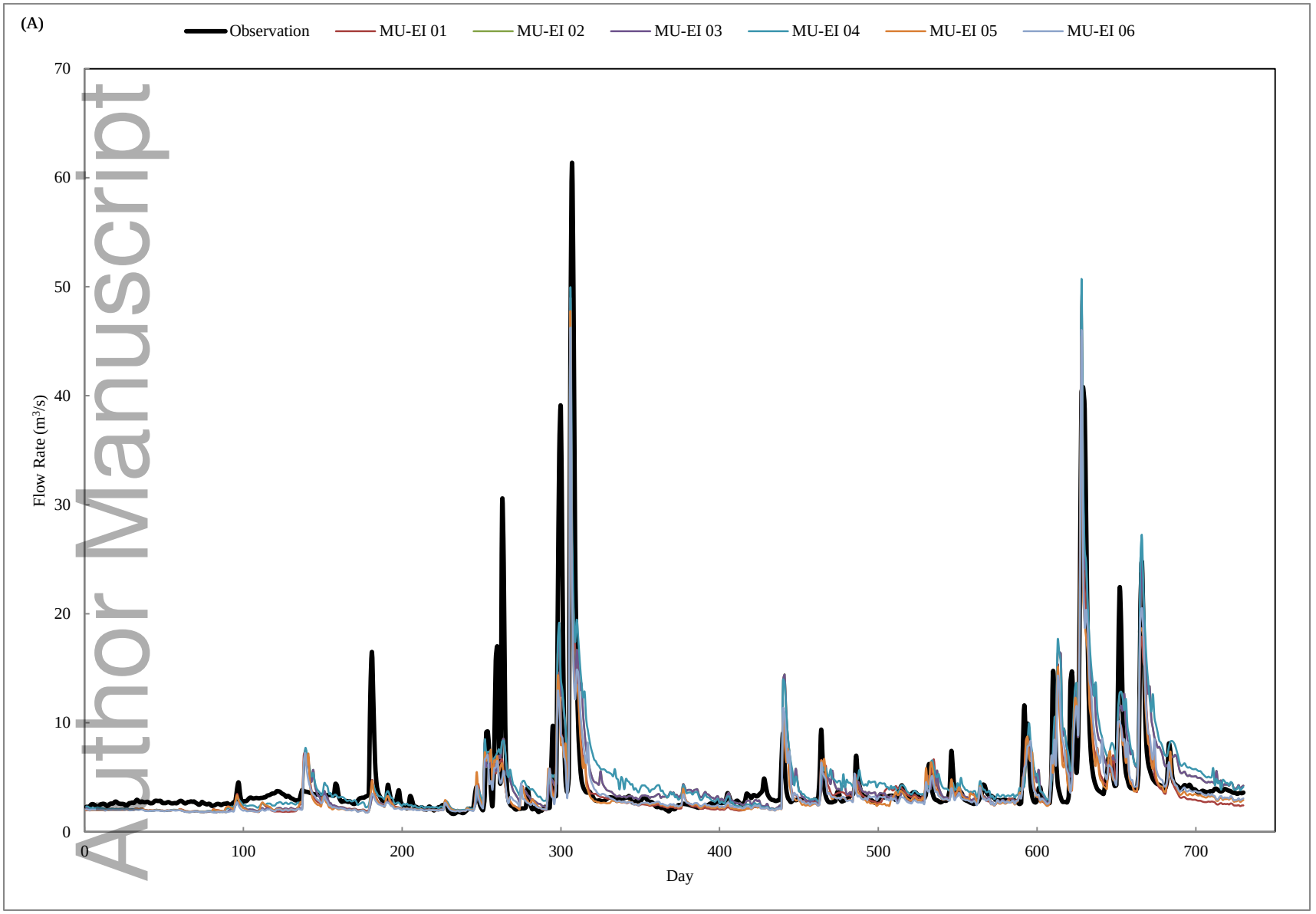

Author Manuscript

1
2

This article is protected by copyright. All rights reserved

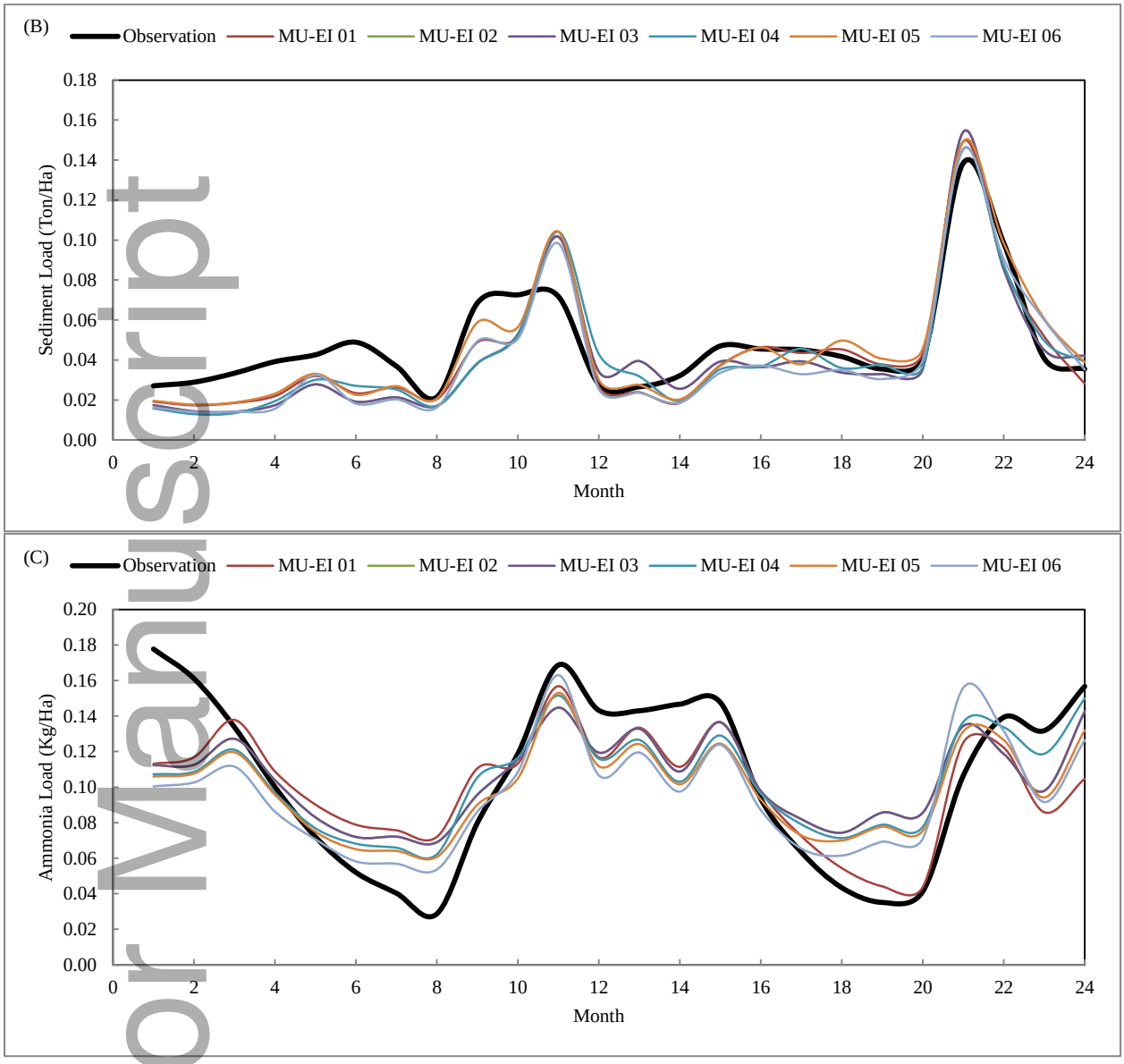

Figure 8. Streamflow, sediment, and NH_4-N predictions (best results from auto-calibration) using MU-EI scheme of all scenarios: (A) Streamflow; (B) Sediment; (C) NH_4-N.

Author Manuscript

This article is protected by copyright. All rights reserved